Benchmarking for the Metamorphic Hand based on a Dimensionality Reduction Model

King's College London: Jie Sun, Ketao Zhang, Jian S. Dai

KTH Royal Institute of Technology: Carl Henrik Ek, Hedvig Kjellstrom, Danica Kragic

1. Introduction

Compared with most of robotic hands, whose fingers can only rotate within a plane because of a fixed palm, the metamorphic hand with a flexible palm improves the adaptably to grasp and manipulate objects with different shapes and reduce the geometric restrictions. The reconfigurable palm was designed based on the metamorphic mechanism, which is a type of mechanisms that have the capability to alter topological configurations along with the changes of the mobility of the mechanisms. The metamorphic robotic hand, which applied the metamorphic mechanism as its palm, expanded the work space of each finger and demonstrated more graspability, adaptability and manipulability for executing different kind of grasp tasks.

This paper evaluates a four-fingered metamorphic robotic hand based on Gaussian process latent variable model[1] (GP-LVM) and compare the results with other robotic hands and grippers. The introduction of this evaluating method is briefly presented followed by building the model the four-fingered metamorphic hand. Results of the proposed robot hand are analyzed in the light of different sampling size of actuated joints and different configurations of the palms.
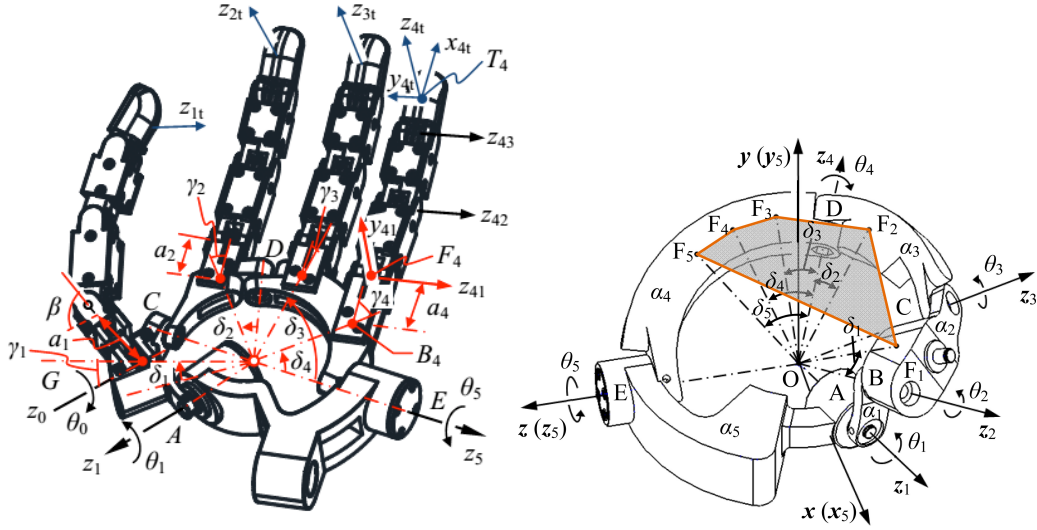
2. Structure of the Metamorphic Hand

2.1 The Design of the Metamorphic Hand

The metamorphic hand, shown in Fig. 1 (a), is made up of a foldable palm and four actuated fingers, i.e. a thumb with four-DOF, and an index finger, a middle finger and a ring finger with three-DOF respectively. The little finger is omitted for decreasing the complexity of design and control because it bends for power grasp normally, which is less important than other fingers from the perspective of functionality. The reconfigurable palm consists of five links which connect to each other as a spherical five-bar linkage mechanism. In order to maximize the rotatability of the spherical five-bar linkage, the angles of link 1 to link 5 are considered as $\alpha_1 = 20°$, $\alpha_2 = 40°$, $\alpha_3 = 70°$ $\alpha_4 = 112°$ and $\alpha_5 = 113°$, which need to satisfy $\alpha_1 + \alpha_2 + \alpha_3 + \alpha_4 + \alpha_5 = 360°$ and the condition, $\alpha_1 + \alpha_2 + \alpha_5 = \alpha_3 + \alpha_4$, presented in [2].

A thumb is mounted to link 2 by a revolute joint, which is similar to the CMC joint of human hands. An index finger is installed on link 3, and the middle finger and ring finger are mounted at link 4. All the fingers have 3 phalanxes that are connected by parallel joints and follow the same design. Different from fingers mounted at a fix palm, the metamorphic hand has the capability to provide the adduction/abduction motions for fingers so as to expand their work space and increase dexterity. Further, the maximum radius of the spherical linkage palm is designed at 50mm in the

light of the size of an adult's hand.

Fig. 1 (a) The design of the metamorphic hand   **(b)** The design of the reconfigurable palm

2.2 Geometric constraints of the metamorphic palm

From the perspective of mechanism, the metamorphic hand can be regarded as a hybrid mechanism consisting of a closed-chain palm and four open-chain fingers. The kinematics of the reconfigurable palm and fingers can be analyzed individually and then combined each other for the whole hand kinematics.

Fig.1 (b) shows the design of the metamorphic palm. Joints A and E are treated as active joints, and joints B, C and D are passive joints. In order to identify the geometric constraints of this reconfigurable palm, coordinate frames are set up in Fig. 3 in such a way that, for all the local coordinate frames of links 1 to 5, they are all centered at point O with z_i-axis aligned with proximal joint of the link i, y_i-axis directed along $z_{i+1} \times z_i$ for i = 1, 2, 3 and 4, and x_i-axis determined by y_i and z_i with the right-hand rule. A global coordinate frame is set up at point O and has its z-axis aligned with joint A and its y axis directed along $z_1 \times z_5$, coinciding with y_5 in Fig. 3. Based on this, given the values of angles θ_1 and θ_5, coordinates of points B, C and D can be obtained in the global coordinate. So do the revolute joints θ_2, θ_3 and θ_4. The analysis of kinematic characteristics of the metamorphic hand was presented in [3].

However, the actuated joints D and C are not independent because of the geometric constraint of the spherical five-bar linkage. From Figure xx, the coordinates of points B and D are calculated in the global coordinate as,

$$P_B = R(y, \alpha_5)\, R(z_1, \theta_1) R(y_1, \alpha_1) k = \begin{bmatrix} \cos\alpha_1 \sin\alpha_5 + \sin\alpha_1 \cos\alpha_5 \cos\theta_1 \\ 0 \\ \cos\alpha_1 \cos\alpha_5 - \sin\alpha_1 \cos\alpha_5 \cos\theta_1 \end{bmatrix}, \tag{1}$$

$$P_C = R(z_5, \theta_5) R(y_4, \alpha_4)\, R(z_4, \theta_4) R(y_3, \alpha_3) k = \begin{bmatrix} \cos\alpha_3 \sin\alpha_4 \cos\theta_5 - \sin\alpha_3(\sin\theta_4 \sin\theta_5 - \cos\alpha_4 \cos\theta_4 \cos\theta_5) \\ \cos\alpha_3 \sin\alpha_4 \sin\theta_5 + \sin\alpha_3(\sin\theta_4 \sin\theta_5 + \cos\alpha_4 \cos\theta_4 \cos\theta_5) \\ \cos\alpha_3 \cos\alpha_4 - \sin\alpha_3 \sin\alpha_4 \cos\theta_4 \end{bmatrix}, \tag{2}$$

$$P_D = R(z, -\theta_5)\, R(y_4, -\alpha_4)k = \begin{bmatrix} \sin\alpha_4 \cos\theta_5 \\ \sin\alpha_4 \sin\theta_5 \\ \cos\alpha_4 \end{bmatrix}, \tag{3}$$

where k is a unit vector as $k = P_E = [0,0,1]^T$.

When assigning the value of angle θ_5, the spherical five-bar linkage mechanism degenerates to a spherical four-bar linkage mechanism. At that time, rotating link 1 will make the spherical four-bar linkage mechanism reach its limited positions when point B, C and D are in the same plane. So,

$$P_d \cdot (P_b \times P_c) = 0, \tag{4}$$

$$P_b \cdot (P_d \times P_c) = 0. \tag{5}$$

The mechanism has two limited position as the link 1 can rotate on both side with respect to link 2. Thus, the value of θ_5 decides the range of that of θ_1, the relation between the two angles can be obtained as,

$$P_B^{\mathrm{T}} \cdot P_A = \cos\alpha_1, \tag{6}$$

$$P_B^{\mathrm{T}} \cdot P_D = \cos(\alpha_2 + \alpha_3), \tag{7}$$

$$P_B^{\mathrm{T}} \cdot P_B = 1. \tag{8}$$

Substituting Eqn. (1) and Eqn. (3) into Eqn. (7) and solving the latter gives the two limited value of angle θ_1 as

$$\theta_1' = \arctan(\frac{Y}{X}) \pm \arccos(\frac{-Z}{\sqrt{X^2 + Y^2}}), \tag{9}$$

where $X = \sin\alpha_4 \cos\theta_5 \cos\alpha_5 \sin\alpha_1 + \sin\alpha_1 \cos\alpha_4 \sin\alpha_5$, $Y = \sin\alpha_1 \sin\alpha_4 \sin\theta_5$ and
$Z = \cos(\alpha_2 + \alpha_3) - \cos\alpha_1 \cos\alpha_4 \cos\theta_5 + \sin\alpha_4 \cos\alpha_1 \cos\theta_5 \sin\alpha_5$.
So the range of θ_1 with a specified θ_5 is,

$$\arctan(\frac{Y}{X}) - \arccos(\frac{-Z}{\sqrt{X^2 + Y^2}}) \leq \theta_1 \leq \arctan(\frac{Y}{X}) + \arccos(\frac{-Z}{\sqrt{X^2 + Y^2}}). \tag{10}$$

Base on Eqn. (10), the range of θ_1 can be calculated by rotating θ_5, whose value changes from

-86° to 86° in terms of the palm design. Taking 1° as the spaced flexion value for θ_5, the range of
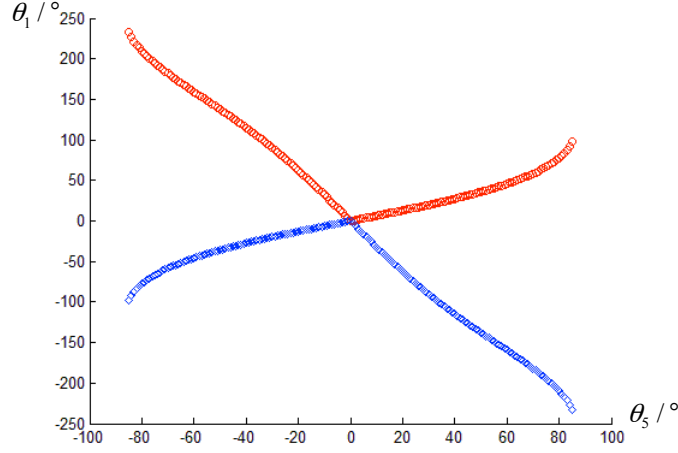
θ_1 is shown in Fig. 2.

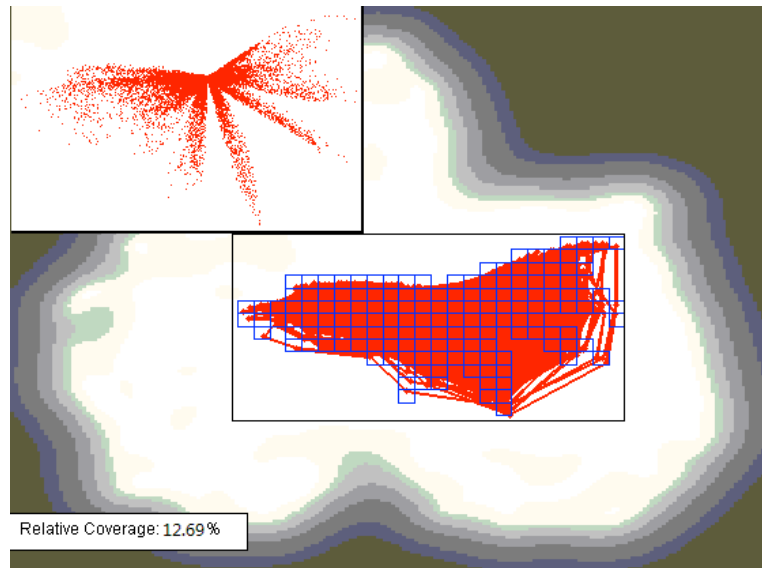**Fig. 2** The range of θ_1 with respect to the changes of θ_5

3. Data generation and Evaluation

3.1 Hand model generation and simplification

According to the requirement of the evaluation method, the metacarpophalangeal (MCP) joint of the middle finger has to be set as the origin. Thus, the link 4, on which the middle finger is located, is fixed as the base. The palm has two degrees of freedom and it is actuated by drive 4 and drive 3, shown in Fig. xxx. The two actuated joints D and C can rotate by different angles to change the configurations of the palm. Specifically, the MCP joint of the index finger will change its position along with the rotation of link 3. Similarly, the coordinate of the carpometacarpal (CMC) joint of the thumb changes with the rotation applied to palm joints D and C. The value of the rotation angles, θ_4 and θ_3, can be calculated based on the rotation of θ_1 and θ_5.

Each finger of the hand has three parallel revolute joints but two active joints, the MCP joint and DIP joint. The PIP joint is coupled with the DIP joints via tendons and share the same rotation angles. Therefore, the metamorphic has 11 DOFs, which leads to a very large sample size. To decrease the complexity and save computing cost, the metamorphic hand is simplified by merging active joints, which results in decreasing the degree of freedom from 11 to 5. Finally, the five left active joints are two palm joints (θ_4 and θ_3), the CMC joint (θ_0) and the MCP joints of the thumb (θ_{11}) and the index finger (θ_{21}), while the other six joints become passive joints. More specifically, the DIP joint of the thumb (θ_{12}) is coupled with its MCP joints (θ_{11}); The DIP joint of index finger (θ_{22}), the MCP joints and DIP joints of the middle finger and the ring finger ($\theta_{31}, \theta_{32}, \theta_{41}$ and θ_{42} respectively) are all coupled with the MCP joint of the index finger (θ_{21}).

The value of θ_0, θ_{11} and θ_{21} ranges from 0 to 80° and 9 equally spaced samples were taken from that range, where $\theta_{(1)}$=0 is finger opened and $\theta_{(9)}$=80° is finger closed. For the two palm joints, θ_4 and θ_3, are assigned with 120 sets of value according to the geometric constraints of the palm. Overall, it generates 87480 different hand postures, which are projected to the latent space, shown in Fig. 3.
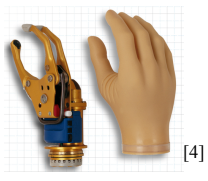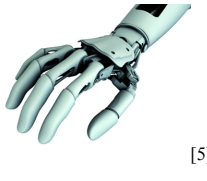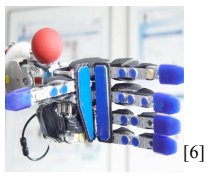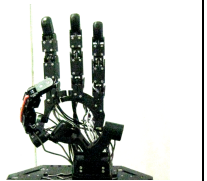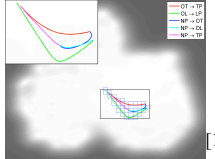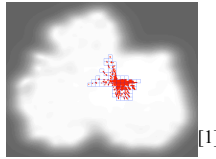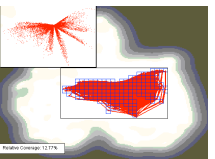
Fig. 3 Projection of the metamorphic hand to the latent space

3.2 Evaluation of the Metamorphic Hand based on AI

The Anthropomorphism Index (AI) is 12.69%. The AI of the metamorphic hand is much higher that of SensorHand[4], Michelangelo Hand[5] and FRH-4 Hand[6], illustrated in Form 1. In particular, the value of the metamorphic hand is nearly 2.5 times as that of FRH-4 Hand on the basis of same number of DOFs but different DOFs in palms. While the palm of the metamorphic hand has 2 DOFs and that of FRH-4 Hand only has 1 DOF.

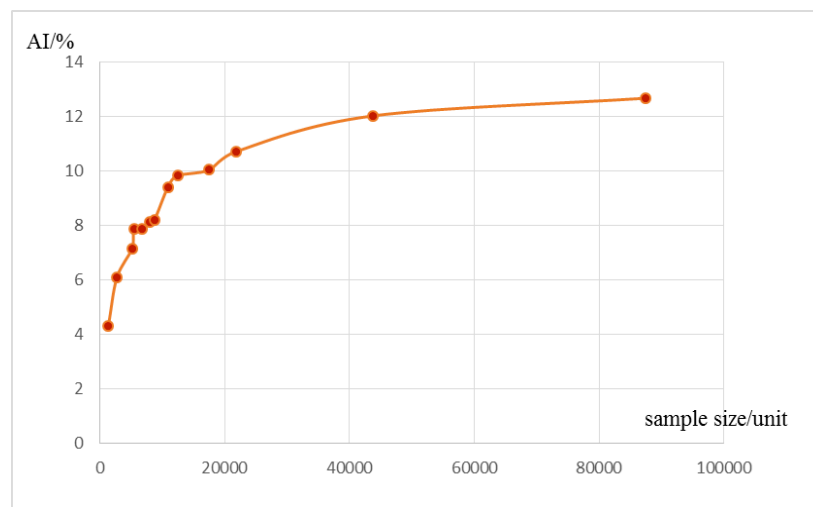Form 1 The AI of four robotic hands evaluated by the toolbox

Hand	Otto Bock SensorHand	Otto Bock Michelangelo Hand	FRH-4 Hand	The metamorphic Hand
Picture	[4]	[5]	[6]	
Fingers	3	5	5	4
Palm DOFs, (All DOFs)	0, (1)	0, (2)	1, (5)	2, (5[1])
Latent space projection	[1]	[1]	[1]	
Coverage	0.25%[1]	2.8%[1]	5.2%[1]	12.69%

[1] Considering the computing cost, the DOFs of the metamorphic hand decreases from 11 to 5. The active joints are two palm joints, the CMC joint and the MCP joints of the thumb and the index finger.

4. Discussion

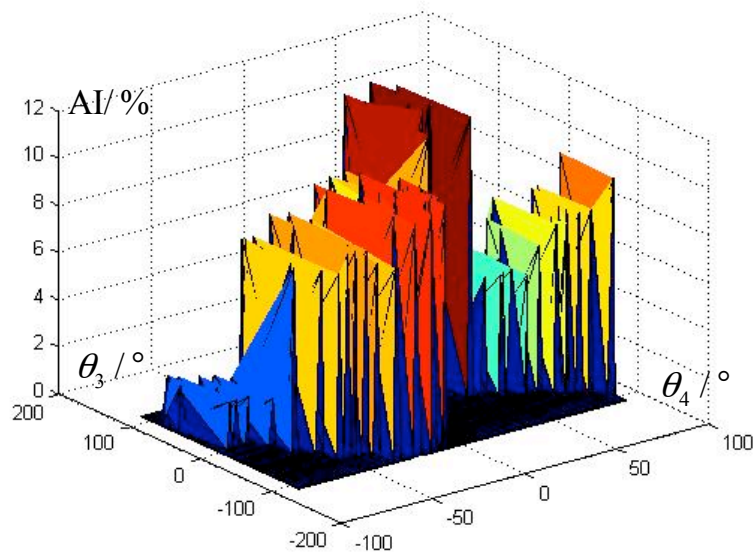**4.1 AI analysis based on different sampling density**

The data of the metamorphic hand are generated by sampling its joint space and calculating the related fingertip poses via forward kinematics. So the sampling density and sample size are the two key factors affecting the value if AI if the number of drives and their range of motion are fixed. Fig. 4 shows the results of AI with different sample density and fixed sample size. The figure shows the changing trend clearly that the larger density of sampling, the higher value of AI. In particular, the increasing trend slowes down with decreasing influence of sampling density. Finallly, the value of AI reaches its upper limit at this sample size.

Fig. 4 The value of AI with fixed sample size and various sampling density

4.2 AI analysis according to different palm configurations.

Based on this dimensionality reduction method, the AI of different palm configurations are capable of being calculated, which contributes to evaluating the functionality of different palm pose and finding the best palm configuration. In other words, the unique palm configuration, which produces the highest AI value, is regarded as the most similar configuring to human hands comparing with other palm poses. Fig. 5 illustrates the relation between the angles of two palm positive joints and the value of AI. The peak of AI value is 11.88% as $(\theta_4, \theta_3) \in \{$ (25.49°, 12.01°), (26.62°, 35.04°), (32.28°, 65.99°), …}. That is to say, in such value of palm rotating angle, the metamorphic hand has the largest graspability.

Fig. 5 The value of AI with different palm configurations

5. Conclusion

References

1. Feix, Thomas, et al. "A metric for comparing the anthropomorphic motion capability of artificial hands." *Robotics, IEEE Transactions on* 29.1 (2013): 82-93.

2. Liu, Yung-Way, and Kwun-Lon Ting. "On the rotatability of spherical N-bar chains." *Journal of Mechanical Design* 116.3 (1994): 920-923.

3. Wei, Guowu, et al. "Kinematic analysis and prototype of a metamorphic anthropomorphic hand with a reconfigurable palm." *International Journal of Humanoid Robotics* 8.03 (2011): 459-479.

4. O. Bock. (2011). SensorHand speed. [Online]. Available: http://www.ottobock.com/cps /rde/xchg/ob_com_en/hs.xsl/3652.html

5. O. Bock. (2011). Otto Bock at the trade fair 2010 Leipzig. [Online]. Available: http://www leipzig.ottobock.de/index.php?id=161&no_cache=1&L=1

6. Gaiser, Immanuel, et al. "A new anthropomorphic robotic hand." *Humanoid Robots, 2008. Humanoids 2008. 8th IEEE-RAS International Conference on*. IEEE, 2008.